



Gamma-rays shielding characteristics of borosilicate glass containing ZnO by using WinXCOM

Recep KURTULUŞ^{1,*} , Taner KAVAS¹ 

¹Afyon Kocatepe University, Faculty of Engineering, Department of Materials Science and Engineering, Afyonkarahisar / TURKEY

Abstract

In this study, the glass system of $(55-x)SiO_2-20B_2O_3-10Na_2O-4MgO-8CaO-3Al_2O_3-xZnO$ where $x: 0, 5, 10, 15, 20$ and 25 wt% were investigated by using WinXCom database. Radiation shielding characteristics of linear attenuation coefficient (LAC), mass attenuation coefficient (MAC), half-value layer (HVL) and mean free path (MFP) parameters of 6 different glass systems were calculated in the photon energy range of 0.015-10 MeV. A comparison for HVL values between heavyweight concrete materials & commercial glasses and our findings was also carried out. Furthermore, some important glass property estimations and viscosity-temperature curve predictions were performed with the use of BatchMaker software. According to the WinXCom calculations, it was found out that LAC and MAC values increased while HVL and MFP values decreased with the increasing ZnO content. Particularly, 25 wt% of ZnO (sample-5) addition ensured to obtain by far the best radiation shielding characteristics at higher photon energies. As a result of the comparison, it was strikingly seen that our glass samples have promising results when compared with heavyweight concrete materials and commercial products. Interestingly, sample-5 can compete even with RS 323 G18 (33 wt% PbO content) in higher photon energies despite its low-density value. Moreover, it was determined that our glass systems were found to have glass formation ability with satisfactory glass properties according to BatchMaker estimate calculations.

Article info

History:
Received: 01.04.2020
Accepted: 07.10.2020

Keywords:
Borosilicate glass,
Radiation shielding,
WinXCom,
Zinc oxide.

1. Introduction

With the developing technology, countless devices with high energy sources have extensively been utilized in medical diagnostics centers, research institutes, non-destructive testing or even in nuclear power plants [1-5]. These devices emit radiation like X-rays or gamma rays through onsite and environment during operation. If such rays are not properly controlled or eliminated, many health problems, for example, radiation sickness or tissue cancer, may occur concerning related rays' dose, intensity, and duration parameters [6], [7] In this way, the use of shielding material is put in place to prevent possible health problems. The prominent shielding material as lead metal stands out due to its high-density (11.34 g/cm^3) against high ionizing radiation energies [8]. However, a search for alternative materials has been continued since the toxicity of lead metal is proved many times, both in environmental and health aspects [9-12] Due to toxicity issues, heavy-weight concrete materials have frequently found use to obtain relatively high-density values and non-toxic substances [13-15]. The interior

walls of medical curing rooms or the surrounding of devices are well-designed via concrete materials for shielding emitting rays. Nevertheless, the application of heavy-weight concrete materials has also been limited due to the risk of cracking during or after hydration processes and operational difficulties onsite [16-18]. Above all, both lead metal and heavy-weight concrete material provide an opaque appearance which means not able to operate under conditions where the transparency is essential (e.g. medical therapy room glass). Therefore, an alternative material having radiation shielding ability as well as transparency appearance has become of interest.

Glasses are outstanding materials that have an amorphous structure [19]. Thanks to its transparency in visible light, compositional flexibility, and environmental friendliness, glass materials have attracted a lot of attention as a radiation shielding material, especially in the past two decades. For this purpose, radiation shielding glass has been researched both theoretically and experimentally by many researchers [20-24]. In the early stages of the studies, researchers focused on the production of lead oxide

*Corresponding author. Email address: rkurtulus@aku.edu.tr
<http://dergipark.gov.tr/csj> ©2020 Faculty of Science, Sivas Cumhuriyet University

(PbO) based glass materials. Yet again, due to the toxicity of lead other high-density-oxides like barium oxide (BaO), bismuth oxide (Bi₂O₃), zinc oxide (ZnO) or the same have been emphasized in the upcoming years as well as nowadays [25-29].

Glass materials can be produced as soda-lime, potash, borate, etc. owing to compositional flexibility. Among other glass systems, borosilicate glasses have an important place [30]. Borosilicate glasses one of these types of glasses and known as available in fabrication at relatively low temperatures, being high thermal shock resistance, having low thermal expansion coefficient and so on [31,32]. Recently, borosilicate glasses have extensively been emphasized because boron oxide (B₂O₃) is very effective on neutron absorption as well as in radiation shielding. With this in mind, radiation shielding characteristics can be improved by adding different high-density-oxides such as Bi₂O₃, Gd₂O₃, BaO or ZnO into the borosilicate glass system. ZnO, which is one of these additives, can be preferred because it has low cost and is not harmful to the environment and health. Besides, it can take roles of a network former or a modifier in the glass system while providing a high refractive index [33].

In literature, studies generally focused on borate, silicate, phosphate and tellurite glasses [34-38]. Several researches were reviewed to explore the shielding characteristics of glass systems. Issa et al. [3] examined zinc tellurite glasses in detail. The change of gamma attenuation by increasing ZnO content was conducted theoretically via WinXCom software and experimentally by different radiation sources. It was concluded that 40 mol.% of the ZnO addition provided the highest MAC and the lowest HVL value. Besides, WinXCom calculations were found to be in good agreement with the experimental measurements. In another, study, Colak et al. [33] studied zinc borate glasses. By making ZnO contribution to the system as 0, 5, 10 and 15 in wt.% the dual roles of ZnO as network former and modifier were emphasized. It was found that with the increasing ZnO addition, the refractive index, as well as the number of non-bridging oxygen, increased while its role of network former was determined by 5 wt.%. Sayyed et al [39] carried out theoretical (WinXCom) calculations of different heavy metal oxide (WO₃, Bi₂O₃, ZnO, etc.) additions in PbCl₂-TeO₂ glass system in the energy range of 0.015 - 15 MeV. They showed that the Z10P20T70 sample containing 10 mol% of ZnO is quite satisfactory compared to some heavy-weight concrete materials and radiation shielding glasses in terms of MAC and HVL values. Likewise, Askin et al. [24] explored gamma ray shielding behavior of the TeO₂-MoO₃-ZnO glass system by theoretically via WinXCom and

Geant4 simulation code. The findings of their study showed that lower TeO₂ amounts diminished radiation shielding effectiveness of glass systems. After all, although a vast number of studies have been conducted to increase radiation shielding characteristics till now there is still a need for searching alternative glass systems to shield harmful ionizing rays.

In general, theoretical studies carried out by researchers do not provide any information about glass properties. In other words, it is not even mentioned whether the glass system put forward in theoretical studies has glass formation ability or not. In this context, it was considered essential to reveal information about the glass properties of this study. A software called BatchMaker® developed by ILIS company ensures reliable prediction of important glass properties and easy drawing of viscosity vs temperature curves [40]. Thus, the functionality of the glass system in the present study will adequately be demonstrated.

In the present study, the glass system of (55-x)SiO₂-20B₂O₃-10Na₂O-4MgO-8CaO-3Al₂O₃-xZnO where x: 0, 5, 10, 15, 20 and 25 wt % were investigated via the WinXCom program. Linear attenuation coefficient (LAC), mass attenuation coefficient (MAC), half-value layer (HVL) and mean free path (MFP) were calculated in 0.015 - 10 MeV photon energy range. Further, some important glass property estimations and viscosity-temperature curve predictions were performed with the BatchMaker software. Details of the studies will be presented in the below sections, accordingly.

2. Materials and Methods

To carry out theoretical calculations, the borosilicate glass design step was initially done. The glass system given in the present study is different from the traditional borosilicate glasses and the percentages of each constituent were originally comprised as listed in Table 1. Along with the increasing ZnO contribution, the decreasing SiO₂ content occurred.

Table 1. Glass system compositions of the present study in wt%.

Sample Code	Na ₂ O	SiO ₂	B ₂ O ₃	CaO	ZnO	MgO	Al ₂ O ₃	Density (g/cm ³)
0	10	55	20	8	0	4	3	2.498
1	10	50	20	8	5	4	3	2.595
2	10	45	20	8	10	4	3	2.698
3	10	40	20	8	15	4	3	2.806
4	10	35	20	8	20	4	3	2.921
5	10	30	20	8	25	4	3	3.043

After completing the glass design, the calculation step was initiated via the WinXCom program. Within the scope of the WinXCom database, MAC can be calculated between 0.001 MeV and 100 GeV. The WinXCom presented by Berger and Hubbel and later developed by Gerward is very beneficial in determining the radiation shielding characteristics of elements, compounds, and mixtures [40].

Beer-Lambert law (Eq. 1) is employed for the calculation of LAC. Eq. 1 is defined as

$$I = I_0 \cdot e^{-\mu t} \tag{1}$$

where *I* and *I*₀ are the transmitted and initial intensities, respectively while μ is linear attenuation coefficient of specimen and *t* is thickness of sample.

The Beer-Lambert equation provides an estimate of the LAC. However, since the material density is a significant factor on the attenuation characteristics, MAC calculation is also required. Here, MAC can be calculated with the aid of Eq. 2

$$\mu_m = \frac{\mu}{\rho} \tag{2}$$

where μ_m is the mass attenuation coefficient while μ represents linear attenuation coefficient and ρ typfies density of specimen.

In radiation shielding material exposed to radiation energy, the distance at which 50% of the incoming energy is attenuated is defined as the half-value layer (HVL). Based on this, the Eq. 3 shows the relation as

$$HVL = \frac{0.693}{\mu} \tag{3}$$

Another parameter, the mean free path (MFP), is directly dependent on the density variable and is related to the mass attenuation coefficient as given in Eq. 4.

$$MFP = \frac{1}{\mu_m} \tag{4}$$

After calculating the radiation shielding parameters, BatchMaker software was applied to draw the viscosity-temperature curves and to calculate some important glass properties. It can be seen screenshots of software to know more about its principle in Figure 1 and Figure 2. Administration of any number of chemical components, raw materials, foreign cullet, and factory cullet or definition of target value, tolerance, saturation and evaporation for each chemical component can be inserted in software [41]. The issue of estimating the glass formation ability and calculating the properties has attracted a lot of attention after the pioneering research was conducted by Fluegel et al. [42,43] which created the groundbreaking statistical modeling in theoretical calculations. Thanks to the BatchMaker software program by ILIS company, the statistical studies were compiled and programmed. Raw material and batch calculations, glass redox calculation, glass properties, viscosity-temperature curve, etc. estimation calculations can easily be carried out. From this point of view, properties of our glass systems were presented.

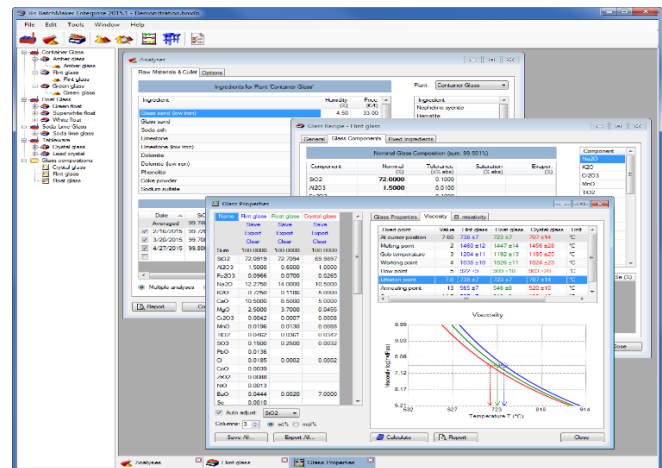


Figure 1. BatchMaker software demonstration screenshot.

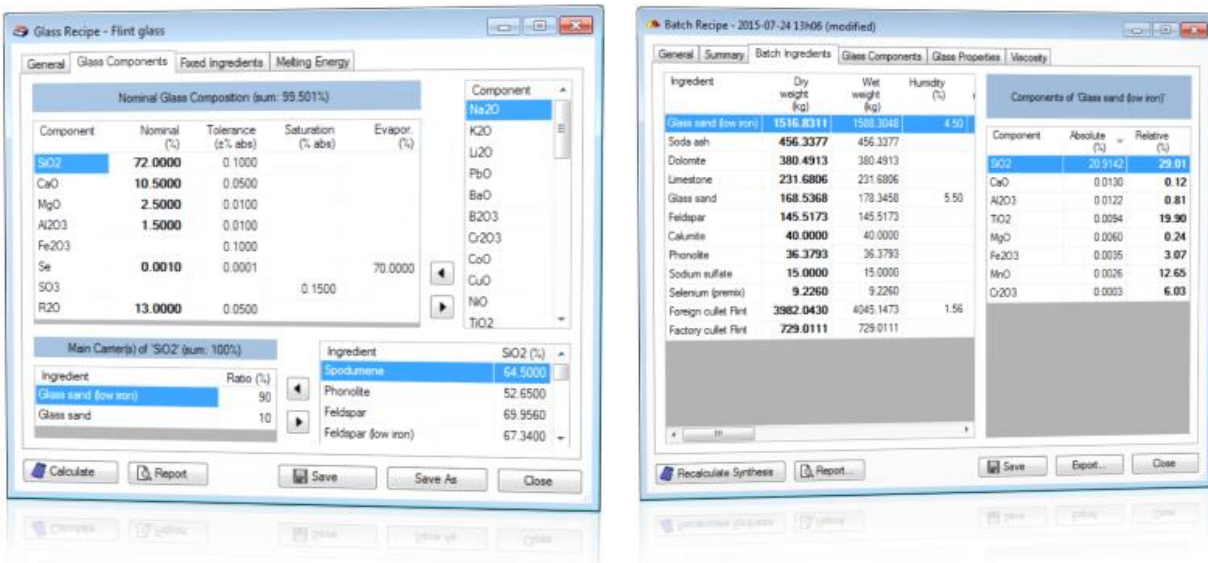


Figure 2. BatchMaker software toolbar screenshots (Left: Glass recipe screen; Right: Batch recipe screen).

3. Results and Discussion

3.1. Radiation shielding characteristics

In this study, the glass system of $(55-x)SiO_2-20B_2O_3-10Na_2O-4MgO-8CaO-3Al_2O_3-xZnO$ where $x: 0, 5, 10, 15, 20$ and 25 wt% were explored via the WinXCom program. *LAC*, *MAC*, *HVL*, and *MFP* parameters were calculated via the WinXCom program in the photon energy range of 0.015 - 10 MeV. *LAC* and *MAC* results were revealed in Figure 3 and Figure 4, respectively. It is obvious that *LAC* and *MAC* increase with the increasing ZnO content. According to the both figures, *LAC* and *MAC* values are very large in low energy regions (e.g. 0.015 to 0.01 MeV) and drops off with the increasing energy (e.g. 1 to 10 MeV). These movements can be explained by three well-known photon interaction matters. In the lower energy regions

photoelectric effect is observed while Compton scattering and pair production processes generate in the medium and higher energies, respectively. Our findings are also in good agreement with several studies conducted by [6,29,44]. Since the ZnO addition paves the way for density increase from 2.498 to 3.043 g/cm³ in the glass system, both *LAC* and *MAC* parameters increase. This is due to the fact that Zn (Z: 30) replaces Si (Z: 14) in the glass matrix. One can state that sample-5 having 25 wt% of ZnO contribution clearly resulted in highest *LAC* and *MAC* values. In particular, we found that the highest ZnO addition improved the radiation shielding characteristics at higher radiation energy levels (greater than 1 MeV). That means, gamma rays can easily be attenuated to the lower values in comparison to remaining glass designs.

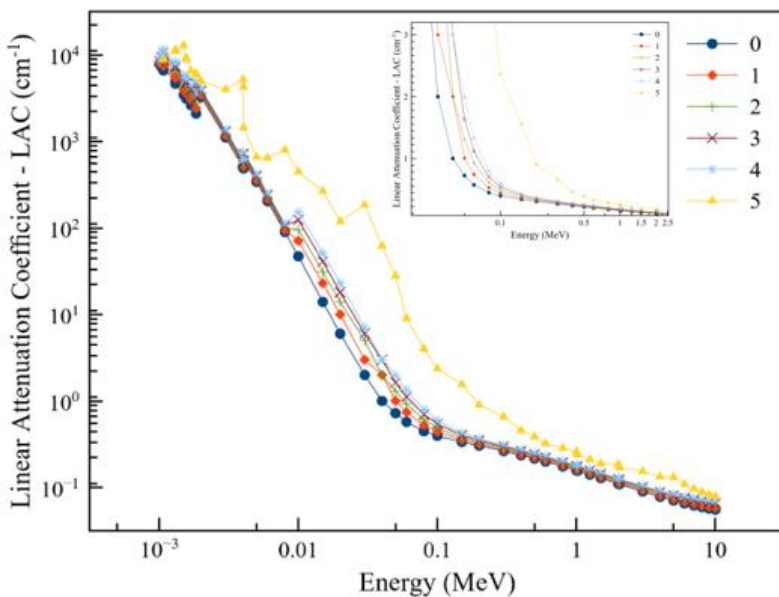


Figure 3. Linear attenuation coefficient for glass systems in the energy range 0.015 to 10 MeV.

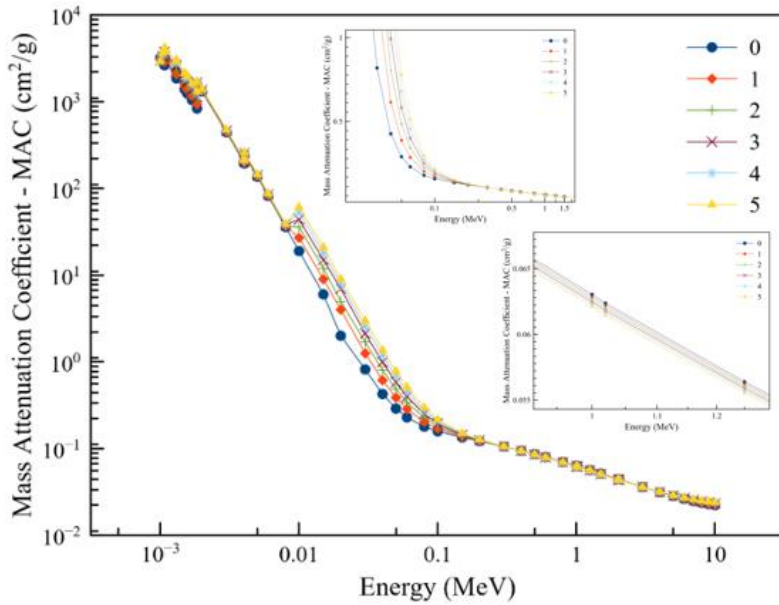


Figure 4. Mass attenuation coefficient for glass systems in the energy range 0.015 to 10 MeV.

On the other hand, the calculations of *HVL* and *MFP* parameters, which are important in terms of thickness value, were presented in Figure 5 and Figure 6, respectively. As known well, the lower the *HVL* and *MFP* values the higher the effectiveness of radiation shielding will [28]. In this respect, both the *HVL* and *MFP* thickness values decrease with the increasing amount of ZnO. Also, as the photon energy increase up to 10 MeV *HVL* values increase. For example, sample-0 at 1 MeV energy, the thickness value is calculated as 4.40 cm, while the increasing ratio of ZnO content in samples 1 - 5 yield 4.25, 4.10, 3.95, 3.81 and 3.66 cm

HVL values, respectively. Substantially, a significant decrease in *HVL* value up to 10 wt% contribution is not observed however, the value decreases considerably when 25 wt% ZnO contribution is employed. Similarly, *MFP* value decreases with increasing ZnO addition. For instance, sample-0 at 2 MeV energy shows a *MFP* value of 7.79 cm, while sample-5 ensures a value of 6.49 cm. Owing to 25 wt% of ZnO addition, the *MFP* value is reduced by 16%, thus improving the radiation shielding characteristics of the glass system.

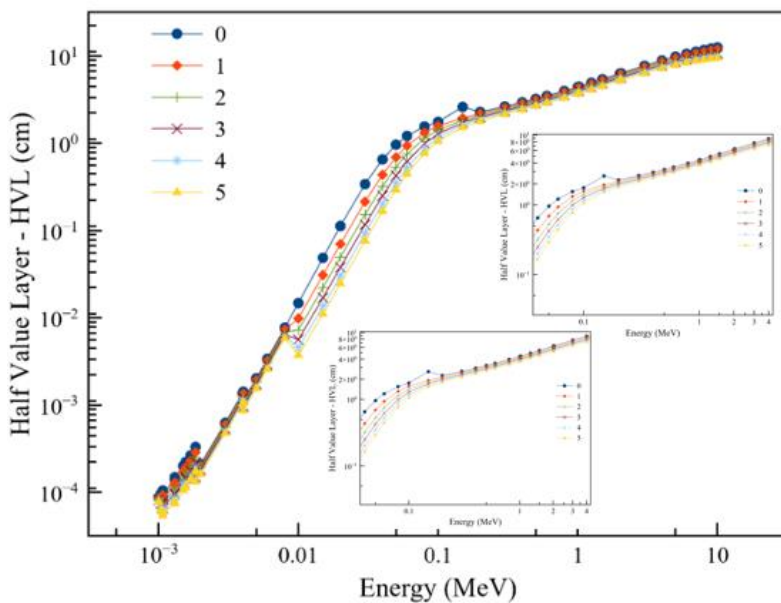


Figure 5. Half value layer for glass systems in the energy range 0.015 to 10 MeV.

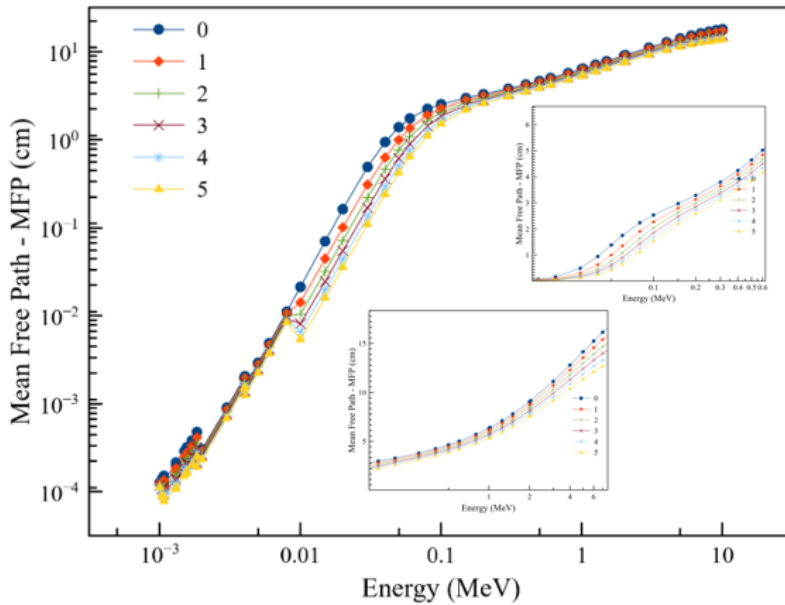


Figure 6. Mean free path for glass systems in the energy range 0.015 to 10 MeV.

3.2. Comparison of the present study with others

In the previous part, WinXCom calculations were evidently presented. In order to make sense of given results above we compared *HVL* values at 0.662 and 1.250 MeV energies relating to some heavyweight concrete materials [45], commercial window glass [46] and commercial radiation shielding glasses [47] and our findings as summarized in Table 2. For heavyweight concrete materials, density values can be increased with different additives, and thus *HVL* values can be decreased, accordingly. To give an example, steel-reinforced concrete has *HVL* value of 2.32 cm whereas standard concrete ensures 3.88 cm at the energy level of 0.662 MeV. In our study, the lowest value for *HVL* was achieved as 2.82 cm with sample-5. At this point, it is critical to say that steel-reinforced concrete material has a greater density value compared to sample-5. On the other hand, it is more significant to compare our glass samples with commercially available ones. Here, the first attention can be drawn on the commercial window glass. That is, *HVL* value is found as 4.73 cm for that glass while all samples of the present study have higher values at 0.662 and 1.250 MeV energies. Moreover, the second attention should be pointed out on commercial RS series glasses produced by Schott company. Of these, RS 253 and RS 253 G18 series do not contain lead oxide (PbO), while the remainings constitute PbO content as 33%, 45%, and 71%, respectively. In this respect, our lead-free glass samples have lower *HVL* values than that of Schott's lead-free ones at both energy levels however, lead-

based glasses of Schott company has relatively lower *HVL* values. Interestingly, despite *HVL* values of sample-5 is found to be greater than RS 323 G18 at 0.662 MeV it achieves a lower *HVL* value when the energy level is increased to 1.25 MeV. In addition to this, sample-4 can compete with RS 323 G18 in terms of *HVL* values at higher energy levels. Therefore, it can be deduced that sample-4 and sample-5 yield lower *HVL* values at higher energies compared to commercially available RS 323 G18 lead-added glass. This phenomenon improves the radiation shielding effectiveness of our glass systems. Not surprisingly, RS 360 and RS 520 products possess slightly lower *HVL* values against our glass samples, because higher amounts of PbO give rise to a higher density of glass system. As a result, it is strikingly seen that our glass samples have promising results when compared with heavy concrete materials and commercial products.

Table 2. Half value layer of some heavyweight concretes, commercial glasses and our glass systems.

Density (g/cm ³)	Shielding Material	Energy (MeV)	
		0.662	1.250
2.40	Standard Concrete	3.88	-
2.50	Hematite Serpentine Concrete	3.62	-
2.90	Ilmenite Limonite Concrete	3.19	-
4.00	Steel Reinforced Concrete	2.32	-
2.50	Commercial Window Glass	4.73	-
2.50	RS 253	3.65	4.95
2.52	RS 253 G18	3.65	4.95
3.26	RS 323 G18	2.48	3.85
3.60	RS 360	2.17	3.30
5.18	RS 520	1.39	2.31
2.50	Sample 0	3.48	4.45
2.60	Sample 1	3.36	4.29
2.70	Sample 2	3.24	4.14
2.81	Sample 3	3.12	4.00
2.92	Sample 4	3.00	3.85
3.04	Sample 5	2.89	3.71

“-“ means not available information.

3.3. BatchMaker software estimate calculations

After comparing glass systems with different materials, the estimation calculations performed via BatchMaker software. Thermal expansion coefficient, density, refractive index, Young's modulus, and liquidus temperature values of glass systems were listed in Table 3. Values related to commercial soda-lime glass (SLS) are also presented in order to make sense of the properties included. With the increasing amount of ZnO, the thermal expansion coefficient, density, refractive index, and liquidus temperature increased whereas Young's modulus decrease. In glass

materials, a high thermal expansion coefficient allows low melting temperature and provides low-cost production. Likewise, having a high refractive index and density value paves the way for its use in radiation shielding applications. As well-known, the high density (5.61 g/cm³) and high refractive index (n = 2.0034) of ZnO can provide to improve radiation shielding properties. Although high liquidus temperature is not desired in glass materials, it is seen that increased ZnO additive causes this situation. Further, our glass systems demonstrate better glass properties rather than SLS glasses.

Table 3. Some important glass properties of our glass systems calculated via BatchMaker software.

Glass Property	Unit	0	1	2	3	4	5	SLS
Thermal expansion	10 ⁻⁶ /K	7.16	7.25	7.34	7.43	7.53	7.63	9.35
Density	g/cm ³	2.498	2.595	2.698	2.806	2.921	3.043	2.481
Refractive index		1.518	1.521	1.52	1.527	1.531	1.535	1.519
Young's modulus	GPa	67.4	66.17	64.5	62.32	59.65	56.41	71.8
Liquidus temperature	°C	1025	1031	1036	1041	1046	1052	1010

The relationship between viscosity and temperature is very significant for glass materials. Viscosity is defined as the resistance of fluidity to flow and differs with the change in fluidity with temperature. Based on

the viscosity-temperature curve approach developed by Lakatos et al. [48] within the scope of the BatchMaker software, the results given in Figure 7 were drawn.

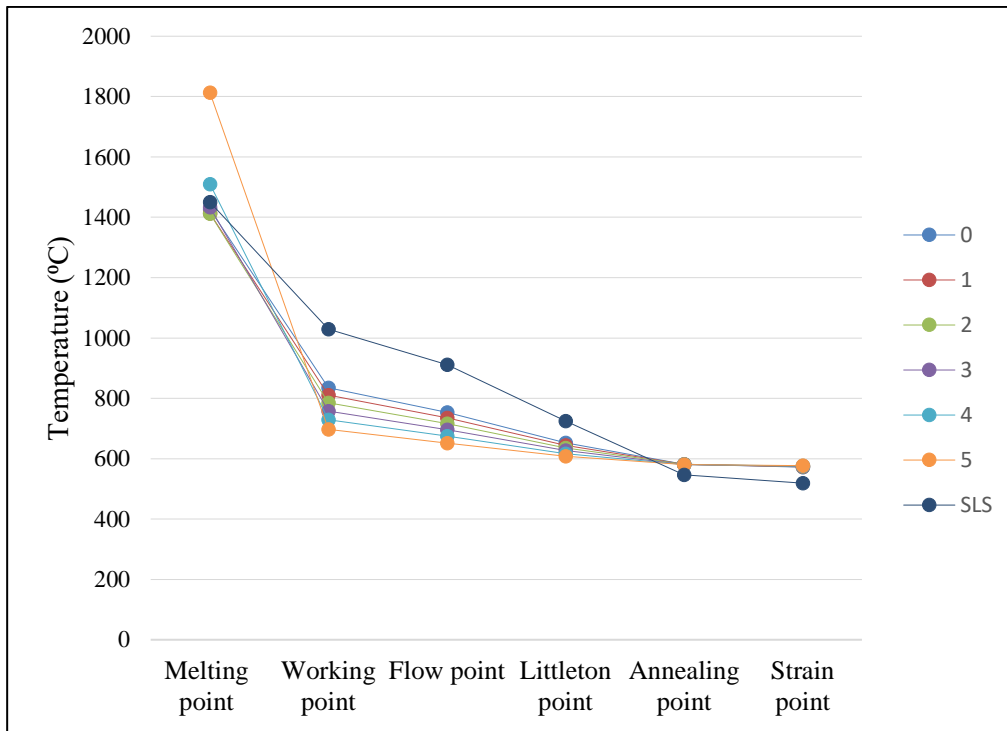


Figure 7. Viscosity vs. Temperature curves for our glass systems drawn via BatchMaker software.

Each point given in the table represents a fixed point for determining flow characteristics. The fixed points can be followed as 2, 4, 5, 7.6, 13 and 14.5 Poise for melting, working, flow, littleton, annealing, and strain points, respectively. In lower content of ZnO in glass systems, the melting point seems to be relatively lower, however as the amount of ZnO is greater than 10 wt%, the melting point is dramatically increased. This can be associated with the network former role of ZnO in the glass system as well as considering the higher melting point of ZnO, namely 1975 °C. Additionally, all-glass systems present similar curves to each other, but there are noticeable differences in melting, working and flow points. Contrarily, SLS glass shows a slightly different curve with regards to our glass samples. That is to say, lower melting point and higher working & flow points are effectual for SLS glass. Consequently, it can be concluded that our glass systems achieve a good viscosity-temperature curve and glass formation ability.

4. Conclusions

The glass system of $(55-x)SiO_2-20B_2O_3-10Na_2O-4MgO-8CaO-3Al_2O_3-xZnO$ where $x = 0, 5, 10, 15, 20$ and 25 wt% were investigated via the WinXCom program in this study. The density of glass systems increased with increasing content of ZnO owing to the higher molecular weight of ZnO in the glass matrix. It was deduced that higher content of ZnO acts as the

network former rather than a modifier role. The linear attenuation coefficient (*LAC*), mass attenuation coefficient (*MAC*), half-value layer (*HVL*) and mean free path (*MFP*) parameters were calculated via WinXCom in the range of 0.015 to 10 MeV photon energies. The findings showed that *LAC* and *MAC* values increased with the increasing ZnO addition, but decreased with increasing photon energy. Further, *HVL* and *MFP* values diminished as the concentration of ZnO increased in glass systems. Hence, the required thickness for shielding material design was figured out. In particular, sample-5 has promising results when compared to some heavyweight concrete materials (*hematite-serpentine* or *ilmenite-limonite*) and commercially available ones (*RS253*, *RS 253 G18*, and *RS 323 G18*). Interestingly, the authors reported that sample-5 can compete with RS 323 G18 (33 wt% PbO content) in higher photon energies despite its low-density value. Moreover, some important glass property estimations and viscosity vs temperature curve predictions were carried out via BatchMaker software to prove glass formation ability. It was pointed out that our glass systems can be fabricated and shows good glass formation ability.

Conflicts of interest

The authors would like to state that there is no conflict of interest.

References

- [1] Kaur P., Singh D. and Singh T., Heavy metal oxide glasses as gamma rays shielding material, *Nucl. Eng. Des.*, 307 (2016) 364–376.
- [2] Lakshminarayana G. *et al.*, Vibrational, thermal features, and photon attenuation coefficients evaluation for $\text{TeO}_2\text{-B}_2\text{O}_3\text{-BaO-ZnO-Na}_2\text{O-Er}_2\text{O}_3\text{-Pr}_6\text{O}_{11}$ glasses as gamma-rays shielding materials, *J. Non. Cryst. Solids*, 481 (2018) 568–578.
- [3] Issa S. A. M., Sayyed M. I. and Kurudirek M., Study of gamma radiation shielding properties of ZnO-TeO_2 glasses, *Bull. Mater. Sci.*, 40 (2017) 841–857.
- [4] Lakshminarayana G. *et al.*, Investigation of structural, thermal properties and shielding parameters for multicomponent borate glasses for gamma and neutron radiation shielding applications, *J. Non. Cryst. Solids*, 471 (2017) 222–237.
- [5] Tijani S. A. and Al-Hadeethi Y., The influence of TeO_2 and Bi_2O_3 on the shielding ability of lead-free transparent bismuth tellurite glass at low gamma energy range, *Ceram. Int.*, 45 (2019) 23572–23577.
- [6] Dong M. G. *et al.*, Investigation of gamma radiation shielding properties of lithium zinc bismuth borate glasses using XCOM program and MCNP5 code, *J. Non. Cryst. Solids*, 468 (2017) 12–16.
- [7] Kaur P., Singh K. J., Thakur S., Singh P., and Bajwa B. S., Investigation of bismuth borate glass system modified with barium for structural and gamma-ray shielding properties, *Spectrochim. Acta - Part A Mol. Biomol. Spectrosc.*, 206 (2019) 367–377.
- [8] Wani A. L., Ara A., and J. Usmani A., Lead toxicity: A review, *Interdiscip. Toxicol.*, 8 (2015) 55–64.
- [9] Verma S., Sanghi S. K., and Amritphale S. S., Development of Advanced, Non-toxic, X-ray Radiation Shielding Glass Possessing Barium, Boron Substituted Kernerupine Crystallites in the Glassy Matrix, *J. Inorg. Organomet. Polym. Mater.*, 28 (2018) 35–49.
- [10] Tijani S. A. *et al.*, Radiation shielding properties of transparent erbium zinc tellurite glass system determined at medical diagnostic energies, *J. Alloys Compd.*, 741 (2018) 293–299.
- [11] Hulbert S. M. and Carlson K. A., Is lead dust within nuclear medicine departments a hazard to pediatric patients?, *J. Nucl. Med. Technol.*, 37 (2009) 170–172.
- [12] Millstone E. and Russell J., Lead toxicity and public health policy, *J. R. Soc. Health*, 115 (1995) 347–350.
- [13] Oto B., Gür A., Kaçal M. R., Doğan B. and Arasoglu A., Photon attenuation properties of some concretes containing barite and colemanite in different rates, *Ann. Nucl. Energy*, 51 (2013) 120–124.
- [14] Zorla E. *et al.*, Radiation shielding properties of high performance concrete reinforced with basalt fibers infused with natural and enriched boron, *Nucl. Eng. Des.*, 313 (2017) 306–318.
- [15] Yilmaz E., Baltas H., Kiris E., Ustabas I., Cevik U., and El-Khayatt A. M., Gamma ray and neutron shielding properties of some concrete materials, *Ann. Nucl. Energy*, 38 (2011) 2204–2212.
- [16] Pomaro B., A Review on Radiation Damage in Concrete for Nuclear Facilities: From Experiments to Modeling, *Model. Simul. Eng.*, 2016 (2016).
- [17] Horszczaruk E., Sikora P., and Zaporowski P., Mechanical properties of shielding concrete with magnetite aggregate subjected to high temperature, *Procedia Eng.*, 108 (2015) 39–46.
- [18] Lee C. M., Lee Y. H., and Lee K. J., Cracking effect on gamma-ray shielding performance in concrete structure, *Prog. Nucl. Energy*, 49 (2007) 303–312.
- [19] Shelby James E, Introduction to Glass Science and Technology Chapter 1., 2. ed., 2006, 1–6.
- [20] Al-Hadeethi Y. and Sayyed M. I., Analysis of borosilicate glasses doped with heavy metal oxides for gamma radiation shielding application using Geant4 simulation code, *Ceram. Int.*, 45 (2019) 24858–24864.
- [21] Singh V. P. *et al.*, Gamma-ray and neutron shielding efficiency of Pb-free gadolinium-based glasses, *Nucl. Sci. Tech.* 27:103 (2016).

- [22] Singh K. J., Kaur S. and Kaundal R. S., Comparative study of gamma ray shielding and some properties of PbO-SiO₂-Al₂O₃ and Bi₂O₃-SiO₂-Al₂O₃ glass systems, *Radiat. Phys. Chem.*, 96 (2014) 153–157.
- [23] Kaewkhao J., Pokaipisit A. and Limsuwan P., Study on borate glass system containing with Bi₂O₃ and BaO for gamma-rays shielding materials: Comparison with PbO, *J. Nucl. Mater.*, 399 (2010) 38–40.
- [24] Askin A., Dal M., Investigation of The Gamma Ray Shielding Behaviour of (90-x)TeO₂- xMoO₃-10ZnO Glass System Using Geant4 Simulation Code and WinXCOM Database, *Cumhur. Sci. J.*, 40 (2019) 742-752.
- [25] Kirdsiri K., Kaewkhao J., Pokaipisit A., Chewpraditkul W. and Limsuwan P., Gamma-rays shielding properties of xPbO:(100-x)B₂O₃ glasses system at 662 keV, *Ann. Nucl. Energy*, 36 (2009) 1360–1365.
- [26] Singh N., Singh K. J., Singh K. and Singh H., Comparative study of lead borate and bismuth lead borate glass systems as gamma-radiation shielding materials, *Nucl. Instruments Methods Phys. Res. Sect. B Beam Interact. with Mater. Atoms*, 225 (2004) 305–309.
- [27] Kaewjaeng S., Kaewkhao J., Limsuwan P. and Maghanemi U., Effect of BaO on optical, physical and radiation shielding properties of SiO₂-B₂O₃-Al₂O₃-CaO- Na₂O glasses system, *Procedia Eng.*, 32 (2012) 1080–1086.
- [28] Waly E. S. A., Fusco M. A., and Bourham M. A., Gamma-ray mass attenuation coefficient and half value layer factor of some oxide glass shielding materials, *Ann. Nucl. Energy*, 96 (2016) 26–30.
- [29] Sayyed M. I., Elmahroug Y., Elbashir B. O. and Issa S. A. M., Gamma-ray shielding properties of zinc oxide soda lime silica glasses, *J. Mater. Sci. Mater. Electron.*, 28 (2017) 4064–4074.
- [30] Mauro J. C., Philip C. S., Vaughn D. J., and Pambianchi M. S., Glass science in the United States: Current status and future directions, *Int. J. Appl. Glas. Sci.*, 5 (2014) 2–15.
- [31] Sayyed M. I., Lakshminarayana G., Dong M. G., Ersundu M. Ç., Ersundu A. E. and Kityk I. V., Investigation on gamma and neutron radiation shielding parameters for BaO/SrO-Bi₂O₃-B₂O₃ glasses, *Radiat. Phys. Chem.*, 145 (2018) 26–33.
- [32] Kumar V., Pandey O. P., and Singh K., Structural and optical properties of barium borosilicate glasses, *Phys. B. Condens. Matter.*, 405 (2010) 204–207.
- [33] Cetinkaya Colak S., Akyuz I., and Atay F., On the dual role of ZnO in zinc-borate glasses, *J. Non. Cryst. Solids*, 432 (2016) 406–412.
- [34] Saeed A., Elbashar Y. H., and El Shazly R. M., Optical properties of high density barium borate glass for gamma ray shielding applications, *Opt. Quantum Electron.*, 48 (2016) 1–10.
- [35] Kurtuluş R. and Kavas T., An Investigation on Usability of Waste Container Glass with Gd₂O₃ and La₂O₃ Addition in Radiation Shielding Applications, *AKU J. Sci. Eng.*, 19 (2019) 219-224.
- [36] Saudi H. A., Lead Phosphate Glass Containing Boron and Lithium Oxides as a Shielding Material for Neutron- and Gamma Radiation, *Appl. Math. Phys.*, 1 (2013) 143–146.
- [37] El-Mallawany R. and Sayyed M. I., Comparative shielding properties of some tellurite glasses: Part 1, *Phys. B. Condens. Matter.*, 539 (2017) 133–140.
- [38] El-Mallawany R., Sayyed M. I., and Dong M. G., Comparative shielding properties of some tellurite glasses: Part 2, *J. Non. Cryst. Solids*, 474 (2017) 16–23.
- [39] Sayyed M. I., Çelikkbilek Ersundu M., Ersundu A. E., Lakshminarayana G. and Kostka P., Investigation of radiation shielding properties for MeO-PbCl₂-TeO₂ (MeO: Bi₂O₃, MoO₃, Sb₂O₃, WO₃, ZnO) glasses, *Radiat. Phys. Chem.*, 144 (2018) 419–425.
- [40] NIST XCOM: Element/Compound/Mixture. Available at: <https://physics.nist.gov/PhysRefData/Xcom/html/xcom1.html>.
- [41] ILIS Company BatchMaker Software. Available at: <https://www.ilis.de/en/batchmaker.html>.
- [42] Fluegel A., Glass viscosity based on a global statistical modeling approach, *Glas. Technol. Eur. J. Glas. Sci. Technol. A*, 48 (2007)13–30.
- [43] Fluegel A., Varshneya A. K., Earl D. A., Seward T. P., Oksoy D. and Street P., Improved composition-property relations in silicate glasses Part 1: Viscosity, *Proceedings of the 106th Annual Meeting of the American Ceramic Society, Ceramic Transactions*, 170 (2004) 129-143.

- [44] El-Kameesy S. Y., El-Ghany S. A., El-Hakam Azooz M. A., and El-Gammam Y. A. A., Shielding Properties of Lead Zinc Borate Glasses, *World J. Condens. Matter Phys.*, 03 (2013) 198-202.
- [45] Singh T. and Singh P. S., Partial as Well as Total Photon Interaction Effective Atomic Numbers for Some Concretes, *J. Nucl. Physics, Mater. Sci. Radiat. Appl.*, 1 (2013) 97-105.
- [46] Kaewjang S., Maghanemi U., Kothan S., Kim H. J., Limkitjaroenporn P. and Kaewkhao J., New gadolinium based glasses for gamma-rays shielding materials, *Nucl. Eng. Des.*, 280 (2015) 21–26.
- [47] Radiation Shielding Glasses for Industrial Applications: SCHOTT Advanced Optics. Available at: https://www.schott.com/advanced_optics/english/products/optical-materials/special-materials/radiation-shielding-glasses/index.html.
- [48] C. Lakatos, L. C, J. LG, and S. B, Viscosity-Temperature Relations in the Glass System SiO₂-Al₂O₃-Na₂O-K₂O-CaO-MgO in the Composition Range of Technical Glasses, *Glas. Technol.*,13 (1972).